JAMA Neurology | Original Investigation

Evaluation of Tau Imaging in Staging Alzheimer Disease and Revealing Interactions Between β-Amyloid and Tauopathy

Liang Wang, MD; Tammie L. Benzinger, MD, PhD; Yi Su, PhD; Jon Christensen, BS; Karl Friedrichsen, BS; Patricia Aldea, MS; Jonathan McConathy, MD; Nigel J. Cairns, PhD; Anne M. Fagan, PhD; John C. Morris, MD; Beau M. Ances, MD, PhD

IMPORTANCE In vivo tau imaging may become a diagnostic marker for Alzheimer disease (AD) and provides insights into the pathophysiology of AD.

OBJECTIVE To evaluate the usefulness of [^{18}F]-AV-1451 positron emission tomography (PET) imaging to stage AD and assess the associations among β-amyloid (Aβ), tau, and volume loss.

DESIGN, SETTING, AND PARTICIPANTS An imaging study conducted at Knight Alzheimer Disease Research Center at Washington University in St Louis, Missouri. A total of 59 participants who were cognitively normal (CN) (Clinical Dementia Rating [CDR] score, 0) or had AD dementia (CDR score, >0) were included.

MAIN OUTCOMES AND MEASURES Standardized uptake value ratio (SUVR) of [^{18}F]-AV-1451 in the hippocampus and a priori–defined AD cortical signature regions, cerebrospinal fluid Aβ42, hippocampal volume, and AD signature cortical thickness.

RESULTS Of the 59 participants, 38 (64%) were male; mean (SD) age was 74 (6) years. The [^{18}F]-AV-1451 SUVR in the hippocampus and AD cortical signature regions distinguished AD from CN participants (area under the receiver operating characteristic curve range [95% CI], 0.89 [0.73-1.00] to 0.98 [0.92-1.00]). An [^{18}F]-AV-1451 SUVR cutoff value of 1.19 (sensitivity, 100%; specificity, 86%) from AD cortical signature regions best separated cerebrospinal fluid Aβ42-positive (Aβ+) AD from cerebrospinal fluid Aβ42-negative (Aβ−) CN participants. This same cutoff also divided Aβ+ CN participants into low vs high tau groups. Moreover, the presence of Aβ+ was associated with an elevated [^{18}F]-AV-1451 SUVR in AD cortical signature regions (Aβ+ participants: mean [SD], 1.3 [0.3]; Aβ− participants: 1.1 [0.1]; $F = 4.3$, $P = .04$) but not in the hippocampus. The presence of Aβ+ alone was not related to hippocampal volume or AD signature cortical thickness. An elevated [^{18}F]-AV-1451 SUVR was associated with volumetric loss in both the hippocampus and AD cortical signature regions. The observed [^{18}F]-AV-1451 SUVR volumetric association was modified by Aβ status in the hippocampus but not in AD cortical signature regions. An inverse association between hippocampal [^{18}F]-AV-1451 SUVR and volume was seen in Aβ+ participants ($R^2 = 0.55$; $P < .001$) but not Aβ− ($R^2 = 0$; $P = .97$) participants.

CONCLUSIONS AND RELEVANCE Use of [^{18}F]-AV-1451 has a potential for staging of the preclinical and clinical phases of AD. β-Amyloid interacts with hippocampal and cortical tauopathy to affect neurodegeneration. In the absence of Aβ, hippocampal tau deposition may be insufficient for the neurodegenerative process that leads to AD.

Editorial page 1049

Supplemental content

CME Quiz at jamanetworkcme.com

Author Affiliations: Department of Neurology, Washington University, St Louis, Missouri (Wang, Cairns, Fagan, Morris, Ances); The Charles F. and Joanne Knight Alzheimer's Disease Research Center, Washington University, St Louis, Missouri (Wang, Benzinger, Cairns, Fagan, Morris, Ances); Department of Radiology, Washington University, St Louis, Missouri (Benzinger, Su, Christensen, Friedrichsen, Aldea, Ances); Department of Radiology, University of Alabama, Birmingham (McConathy); The Hope Center for Neurological Disorders at Washington University, St Louis, Missouri (Fagan, Morris, Ances).

Corresponding Author: Beau M. Ances MD, PhD, Department of Neurology, Washington University, 660 S Euclid Ave, PO Box 8111, St Louis, MO 63110 (bances@wustl.edu).

JAMA Neurol. 2016;73(9):1070-1077. doi:10.1001/jamaneurol.2016.2078
Published online July 25, 2016.

Accumulation of β-amyloid (Aβ) and tau proteins, the hallmark pathology of Alzheimer disease (AD), occurs in a spatially ordered manner.[1,2] The spatial spreading of these pathologic proteins is indicative of the temporal progression of AD. Deposition of Aβ initially occurs in widely distributed neocortical areas.[3] The presence of widespread Aβ plaques in these areas marks the beginning of preclinical AD.[4] Tau aggregation in the form of neurofibrillary tangles first appears in the entorhinal cortex.[1] The spreading of neurofibrillary tangles into the neocortex is associated with the transition from the preclinical to clinical phase of AD.[5]

The burden of Aβ in the brain has been measured by cerebrospinal fluid (CSF) Aβ42 and positron emission tomography (PET) amyloid imaging.[6,7] Neurodegeneration has been indexed by CSF tau/phosphorylated tau_{181} ($ptau_{181}$) and brain volumetrics.[8] Stage 1 of preclinical AD is denoted by isolated amyloidosis (decreased CSF Aβ42 or elevated amyloid tracer binding).[9] Stage 2 of preclinical AD is defined by the presence of both amyloidosis and neurodegeneration (increased CSF tau/$ptau_{181}$ or atrophy on magnetic resonance imaging [MRI]).[9]

Recently developed PET tracers, including [^{18}F]-AV-1451, bind to aggregated tau in neurofibrillary tangles.[10-16] Initial work[17-19] has reported that [^{18}F]-AV-1451 binding is elevated in neocortical areas in patients with AD compared with cognitively normal (CN) participants. The topography of AD-related cortical neurodegeneration has been delineated by MRI as the AD cortical signature,[20] in which volumetric loss is correlated with tau burden measured at autopsy[21] or CSF assay.[22] Thus, [^{18}F]-AV-1451 binding in AD cortical signature regions may be useful for staging of AD.

In addition to potential application to disease staging, tau imaging may advance our understanding of the pathophysiology of AD.[15,23] Emerging evidence suggests that Aβ alone is necessary, but not sufficient, for the development of AD.[15,24-26] Specifically, it is hypothesized[25] that Aβ serves as an initiator of a pathogenic cascade that triggers the spread of neurofibrillary tangles and associated neurodegeneration. In addition, neurofibrillary tangles accumulate in the hippocampus and adjacent medial temporal cortices with both aging and AD. Some investigators[27] have argued that hippocampal tauopathy is amplified by Aβ during AD; others[28-30] have suggested that hippocampal neurofibrillary tangle accumulation or neurofibrillary tangle–related hippocampal atrophy occurs independently of Aβ. The ability to perform in vivo imaging of Aβ and tauopathy allows us to study whether Aβ intensifies tauopathy and associated neuronal loss within and beyond the medial temporal lobe.

In the present study, we compared [^{18}F]-AV-1451 binding in the hippocampus and AD cortical signature regions with volumetric measurements (ie, hippocampal volume and AD signature cortical thickness) and with CSF $ptau_{181}$ in discriminating participants with AD from CN participants. We assessed the associations among CSF Aβ42, [^{18}F]-AV-1451 binding, and volumetric measurements and specifically examined whether the interaction between CSF Aβ42 and [^{18}F]-AV-1451 binding affected hippocampal volume or AD signature cortical thickness.

Key Points

Question What is the value of [^{18}F]-AV-1451 positron emission tomography (PET) imaging in staging of Alzheimer disease and revealing interactions between β-amyloid and tauopathy?

Findings A PET imaging study using [^{18}F]-AV-1451 distinguished participants with Alzheimer disease (AD) from those who were cognitively normal. An elevated [^{18}F]-AV-1451 binding was associated with volumetric loss in both the hippocampus and cerebral cortex; however, the observed [^{18}F]-AV-1451 binding–volumetric association was modified by Aβ pathology in the hippocampus but not in AD cortical signature regions.

Meaning Tau PET imaging has potential for staging of AD; Aβ interacts with hippocampal and cortical tauopathy to affect neurodegeneration.

Methods

Participants

Participants were community-living volunteers recruited for longitudinal studies of memory and aging at the Knight Alzheimer Disease Research Center at Washington University, St Louis, Missouri. Recruitment procedures have been published.[31] Participants were eligible for the present study if they completed both [^{18}F]-AV-1451 PET imaging and brain MRI within 12 months of clinical assessment. Individuals were excluded from the present study if they had (1) neurologic, psychiatric, or systemic illness that might affect cognition; (2) an autosomal dominant mutation for AD; or (3) other neurodegenerative disorders (eg, frontotemporal dementia). The Washington University School of Medicine Human Research Protection Office approved this study, with written informed consent obtained from each participant. The participants received financial compensation.

Clinical Assessment and Disease Stage Classification

The participant and an informant underwent separate semistructured interviews conducted by experienced clinicians. The presence or absence of cognitive impairment was determined by assessing whether there was intraparticipant decline from previously attained levels of cognitive function using the Clinical Dementia Rating (CDR) scale, with 0 indicating normal cognition and greater than 0 indicating cognitive impairment.[32] A diagnosis of dementia due to AD was made according to published criteria.[33]

Cerebrospinal fluid levels of Aβ42, total tau, and $ptau_{181}$ were measured in a subset of participants (eMethods in the Supplement). Using a priori–defined cutoffs, the present cohort of participants was classified as either CSF Aβ42 positive (Aβ+) or CSF Aβ42 negative (Aβ−). The application of CSF Aβ42 cutoffs and clinical diagnosis allowed participants to be classified as Aβ− CN, Aβ− AD, Aβ+ CN, or Aβ+ AD.

Structural MRI Acquisition and Processing

Participants underwent scanning with either a Siemens 3-T Trio (n = 14) or Biograph mMR (n = 45) scanner (Siemens Medical

Figure 1. Regional and Vertexwise Associations Between [^{18}F]-AV-1451 Binding and Cortical Thickness

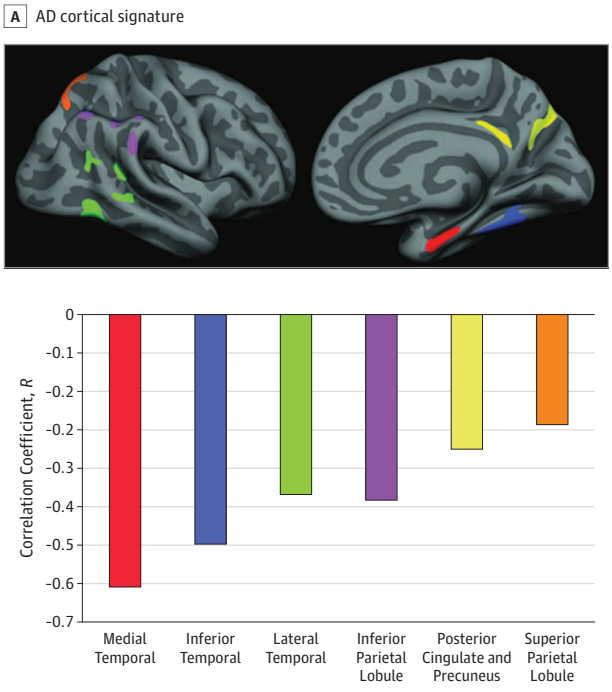

Pearson correlation between [^{18}F]-AV-1451 binding and cortical thickness was assessed for each region of interest that composed the Alzheimer disease (AD) cortical signature (A) and each vertex across the cortical mantle (B). The regional correlation coefficients are showed with a bar graph in an order that is consistent with the hypothetical sequence of neurofibrillary tangles spreading. The color-coded anatomic location of AD cortical signature regions is labeled in the bar graph accordingly. The significance of vertexwise correlation was thresholded at $P < .05$, corrected for multiple comparisons at the cluster level. Both AD cortical signature regions and vertexwise correlation are displayed on the semi-inflated cortical surface of the FreeSurfer average brain, with light gray regions representing gyri and dark gray regions representing sulci.

Systems). Structural scans were processed with FreeSurfer, version 5.30 (http://freesurfer.net/) (eMethods in the Supplement). For each hemisphere, thickness values were obtained from 6 AD signature regions of interest (inset in **Figure 1**A) based on previous work.[22] Cortical thickness was averaged across hemispheres and then across the 6 AD signature regions of interest to generate a single AD signature cortical thickness mean composite score. In addition, hippocampal volume was obtained and adjusted for intracranial volume (eMethods in the Supplement).

[^{18}F]-AV-1451 PET Imaging and Processing

Imaging was performed using a Biograph 40 PET/CT scanner (Siemens Medical Solutions). PET scans were acquired after intravenous administration of approximately 9 to 13 mCi of [^{18}F]-AV-1451. Reconstruction was performed using an ordinary Poisson-ordered subset expectation maximization algorithm (256 × 256 × 109 matrix, 1.34 × 1.34 × 2.03-mm voxels on the Biograph 40 scanner) with random, scatter, attenuation, and decay correction. Dynamic PET images were corrected for interframe motion using in-house software.[34] PET imaging data acquired between 80 and 100 minutes after injection of [^{18}F]-AV-1451 were summed and registered to the participant's MRI space. Voxelwise standardized uptake value ratio (SUVR) was estimated by normalizing the summed PET images by the mean cerebellar cortex intensity. Voxelwise SUVR was not corrected for partial volume effect. The SUVR values from AD cortical signature composite regions and the hippocampus were obtained using a method similar to the one described above for volumetric measurements. Additional processing for vertexwise analysis is provided in the eMethods in the Supplement. In addition, [^{18}F]-AV-1451 has been shown[18] to bind to the target other than tau (ie, off-target binding) in the choroid plexus that might confound the hippocampal PET signal. We used partial volume correction[35] and linear regression approaches to address this confounding effect (eMethods, eResults, eTable 1, and eFigure 1 in the Supplement).

Statistical Analysis

Group differences for hippocampal [^{18}F]-AV-1451 SUVR or volume, AD cortical signature [^{18}F]-AV-1451 SUVR or cortical thickness, and CSF ptau$_{181}$ levels were compared across Aβ− CN, Aβ+ CN, and Aβ+ AD groups using independent, 2-tailed *t* tests. Overall, the Aβ− AD group was excluded from subsequent comparisons because of limited sample size (n = 1). Receiver operating characteristic analyses assessed the ability of hippocampal [^{18}F]-AV-1451 SUVR or volume, AD cortical signature [^{18}F]-AV-1451 SUVR or thickness, and CSF ptau$_{181}$ to distinguish the Aβ+ AD from the Aβ− CN or Aβ+ CN groups. The cutoff for each measurement that best discriminated these groups was selected using the Youden index (ie, a maximum of sensitivity + [specificity − 1]). With regard to differentiating Aβ+ AD from Aβ− CN or from Aβ+ CN, the AUCs were compared between possible measurement pairs (eg, hippocampal [^{18}F]-AV-1451 SUVR vs volume) using a bootstrap test implemented in R, version 3.2.3.[36]

The effect of Aβ status (ie, Aβ+ vs Aβ−) on hippocampal [^{18}F]-AV-1451 SUVR or volume and AD cortical signature [^{18}F]-AV-1451 SUVR or thickness was assessed using general linear models with age and CDR status included as covariates. Associations between [^{18}F]-AV-1451 SUVR and volumetric measurement were evaluated for the hippocampus, AD cortical signature as a whole, and each region of interest that composed the AD cortical signature using Pearson correlations. The modulation of Aβ status on the association between [^{18}F]-AV-1451 SUVR and volumetric measurement was tested sepa-

rately for the hippocampus, AD cortical signature as a whole, and each region of interest within the AD cortical signature using general linear models. Specifically, for each general linear model, the interaction of Aβ status and regional [^{18}F]-AV-1451 SUVR on the volumetric measurement was first tested and reported if confirmed. Otherwise, the independent effect of [^{18}F]-AV-1451 SUVR was reported after adjusting for age and CDR status. Analyses were implemented using SPSS, version 23.0 (IBM), with a statistical threshold for significance of $P < .05$ corrected for multiple comparisons using a false-discovery rate.

Table 1. Demographics of Entire Cohort

Characteristic	Value
No.	59
Age, mean (SD), y	74 (6)
Male, No. (%)	38 (64)
Education, mean (SD), y	16 (2)
MMSE score, mean (SD)[a]	28 (2)
CDR (No. 0/>0), No. (%)[b]	50 (85)/9 (15)

Abbreviations: CDR, Clinical Dementia Rating; MMSE, Mini-Mental State Examination.

[a] The score of the MMSE ranges from 30 (best) to 0 (worst).

[b] The indicators for the CDR are 0 (normal cognition) and greater than 0 (cognitive impairment).

Results

Demographic information of the entire cohort is provided in **Table 1**. Within the subset of participants who had CSF biomarkers (n = 42), the Aβ+ AD group was older than the Aβ− CN group and had lower Mini-Mental State Examination scores (with 30 indicating the best and 0 the worst score) than either the Aβ− CN or Aβ+ CN group (eTable 2 in the Supplement). No group differences were seen for other demographic variables.

The [^{18}F]-AV-1451 SUVR was elevated in both the hippocampal and AD cortical signature regions in Aβ+ AD compared with Aβ+ CN or Aβ− CN participants. Hippocampal volume and AD signature cortical thickness were reduced in Aβ+ AD compared with Aβ+ CN or Aβ− CN participants (**Figure 2**). The CSF ptau$_{181}$ level was increased in the Aβ+ AD compared with the Aβ− CN group but was similar between the Aβ+ AD and Aβ+ CN groups. Relative to Aβ− CN participants, the Aβ+ CN group exhibited an increase in [^{18}F]-AV-1451 SUVR in AD cortical signature regions but not in the hippocampus. The Aβ+ CN group also showed an increase in CSF ptau$_{181}$ compared with Aβ− CN. Both hippocampal volume and AD signature cortical thickness were similar for the Aβ+ CN and Aβ− CN groups.

Receiver operating characteristic analyses assessed the utility of [^{18}F]-AV-1451 SUVR, brain volumetrics, and CSF ptau$_{181}$

Figure 2. Regional [^{18}F]-AV-1451 Binding, Volumetric Measurement, and Cerebrospinal Fluid (CSF) Phosphorylated Tau$_{181}$ (ptau$_{181}$) According to β-Amyloid (Aβ) Status and Clinical Diagnosis

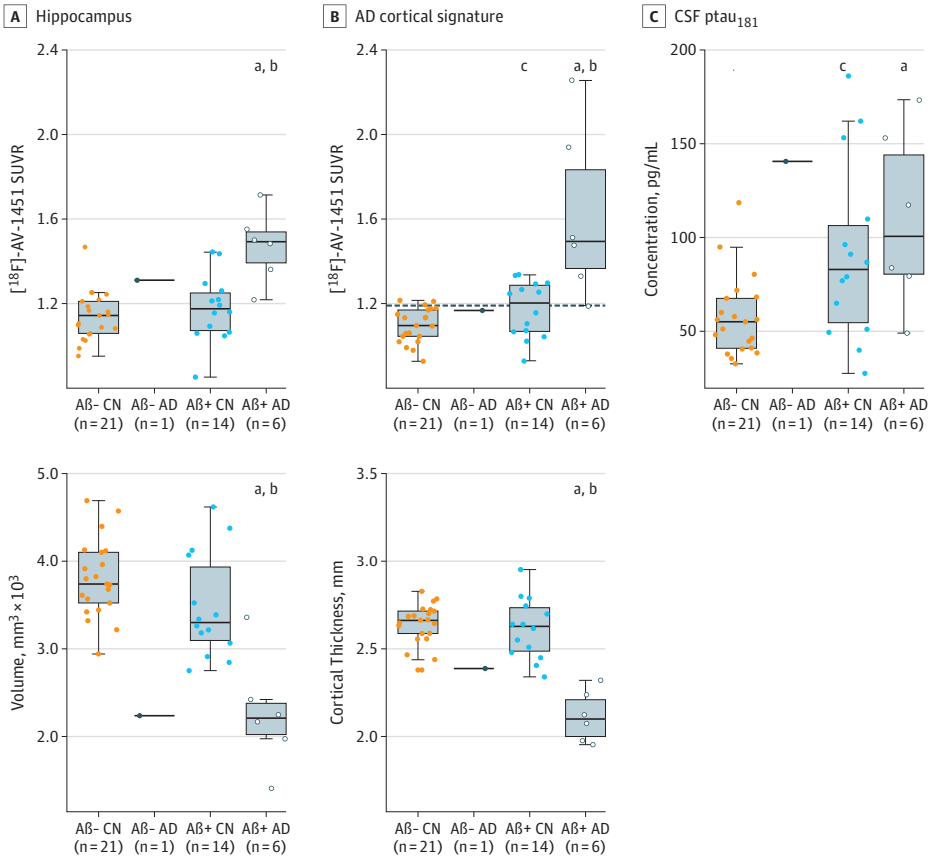

Hippocampal [^{18}F]-AV-1451 binding (ie, standardized uptake value ratio [SUVR]) or volume (adjusted with intracranial volume) (A), Alzheimer disease (AD) signature [^{18}F]-AV-1451 SUVR or cortical thickness (B), and CSF ptau$_{181}$ (C) are presented with individual data points and boxplot showing the range, median, and interquartile range. The dashed line, corresponds to an SUVR of 1.19 derived from the AD cortical signature composite for [^{18}F]-AV-1451 and represents a cutoff that best separated CSF Aβ42-positive (Aβ+) AD from CSF Aβ42-negative (Aβ−) cognitively normal (CN) participants. The Aβ level was measured by CSF assay of Aβ42. Cutoffs for Aβ status (ie, CSF Aβ+ vs Aβ−) were determined from an independent cohort. Group difference in each measurement was compared using a *t* test.

[a] $P < .05$ in comparison between Aβ+ AD vs Aβ− CN.

[b] $P < .05$ in comparison between Aβ+ AD vs Aβ+ CN.

[c] $P < .05$ in comparison between Aβ+ CN vs Aβ− CN.

Table 2. Usefulness of [^{18}F]-AV-1451 Binding, Volumetric Measurement, and CSF ptau$_{181}$[a]

Variable	Aβ− CN vs Aβ+ AD		Aβ+ CN vs Aβ+ AD	
	AUC (95% CI)	Optimal Cutoff (Sensitivity, Specificity)[b]	AUC (95% CI)	Optimal Cutoff (Sensitivity, Specificity)[b]
[^{18}F]-AV-1451 SUVR				
Hippocampus	0.95 (0.87-1.00)	1.36 (83%, 95%)	0.92 (0.79-1.00)	1.36 (83%, 86%)
AD cortical signature	0.98 (0.92-1.00)	1.19 (100%, 86%)	0.89 (0.73-1.00)	1.33 (83%, 86%)
Volumetric measurement				
Hippocampus	0.98 (0.92-1.00)	3420 (86%, 100%)	0.91 (0.71-1.00)	2749 (100%, 83%)
AD cortical signature	1.00 (1.00-1.00)	2.37 (100%, 100%)	1.00 (1.00-1.00)	2.34 (100%, 100%)
CSF ptau$_{181}$	0.86 (0.68-1.00)	79 (83%, 86%)	0.61 (0.34-0.88)	79 (83%, 50%)

Abbreviations: Aβ, β-amyloid; Aβ−, Aβ42 negative; Aβ+, Aβ42 positive; AD, Alzheimer disease; AUC, area under the receiver operating characteristic curve; CN, cognitively normal; CSF, cerebrospinal fluid; ptau$_{18}$, phosphorylated tau; SUVR, standardized uptake value ratio.

[a] The AUC analysis evaluated the accuracy of hippocampal [^{18}F]-AV-1451 binding (SUVR), hippocampal volume, AD cortical signature [^{18}F]-AV-1451 SUVR and thickness, and CSF ptau$_{181}$ in differentiating the Aβ+ AD from the Aβ− CN group or from the Aβ+ CN group. The Aβ level was measured by a CSF fluid assay of Aβ42. Cutoffs for Aβ status (ie, CSF Aβ+ vs Aβ−) were determined in an independent cohort.

[b] The cutoff is the value of the corresponding variable that provided best separation of the groups. For example, 1.36 indicates that the hippocampal SUVR of 1. 36 best separated Aβ− CN from Aβ+ AD.

Figure 3. Associations Among β-Amyloid (Aβ) Status, [^{18}F]-AV-1451 Binding, and Volumetric Measurement

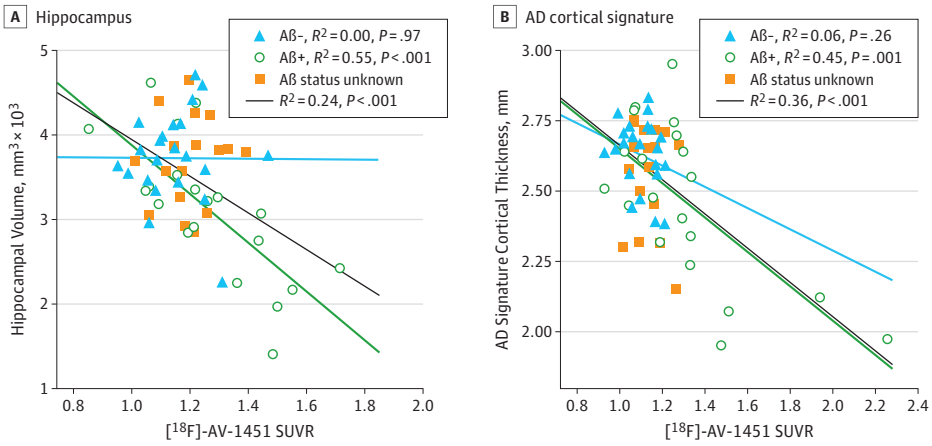

[^{18}F]-AV-1451 binding (standardized uptake value ratio [SUVR]) is plotted against volumetric measurement for the hippocampus (A) and Alzheimer disease (AD) cortical signature regions (B). Linear fitting is presented for the entire cohort (N = 59, black line) and separately for Aβ positive (Aβ+) (n = 20, green line) vs Aβ negative (Aβ−) group (n = 22, blue line). With Aβ status, the slope of linear fitting was significantly different in the hippocampus (P = .01) but not AD cortical signature regions (P > .05) after adjusting for age and Clinical Dementia Rating (CDR) status (CDR 0 vs CDR >0). Aβ+ or Aβ− indicates positive or negative for Aβ biomarker, respectively.

for discriminating the AD from the CN group (**Table 2**). The [^{18}F]-AV-1451 SUVR in the hippocampus and AD cortical signature regions distinguished Aβ+ AD from the Aβ− CN or Aβ+ CN group (area under the receiver operating characteristic curve [95% CI], 0.89 [0.73-1.00] and 0.98 [0.92-1.00], respectively). With regard to the differentiation of Aβ+ AD from Aβ− CN or from Aβ+ CN, differences in the area under the receiver operating characteristic curve were observed only between AD signature cortical thickness (both 1.00 [95% CI, 1.00-1.00]) and CSF ptau$_{181}$ (Aβ− CN vs Aβ+ AD: 0.86 [95% CI, 0.68-1.00]; Aβ+ CN vs Aβ+ AD: 0.61 [95% CI, 0.34-0.88]).

An [^{18}F]-AV-1451 SUVR cutoff of 1.19 within AD cortical signature regions best separated Aβ+ AD from Aβ− CN (sensitivity, 100%; specificity, 86%). This same cutoff also classified Aβ+ CN participants into low vs high tau groups (Figure 2). The Aβ+/low tau CN group had an [^{18}F]-AV-1451 SUVR from AD cortical signature regions that was similar to that in the Aβ− CN group and did not overlap with the SUVR in Aβ+ AD participants. The Aβ+/high tau CN group had [^{18}F]-AV-1451 SUVR from AD cortical signature regions that resembled the lower quartile in the Aβ+ AD group and did not overlap with that of Aβ− CN participants. In addition, a secondary analysis using a gaussian mixture model showed that the Aβ+ CN group contained 2 distributions that reflected the low vs high tau levels in individuals (eResults and eFigure 2 in the Supplement).

We next examined the associations among Aβ status, [^{18}F]-AV-1451 SUVR, and volumetric measurements in the hippocampus and AD cortical signature regions. The [^{18}F]-AV-1451 SUVR in AD cortical signature regions was increased in the Aβ+ participants (mean [SD], 1.3 [0.3]) compared with the Aβ− participants (mean [SD], 1.1 [0.1]; F = 4.3; P = .04) after adjusting for age and CDR status. The presence of Aβ+ was not associated with elevated [^{18}F]-AV-1451 SUVR in the hippocampus after adjusting for age and CDR status. In addition, an effect of Aβ status was not seen for hippocampal volume or AD signature cortical thickness after adjusting for age and CDR status. An inverse relationship was observed between [^{18}F]-AV-1451 SUVR and volumetrics for both the hippocampus (R^2 = 0.24, P < .001) and AD cortical signature regions (R^2 = 0.36, P < .001) (**Figure 3**). We further examined the association between the regional [^{18}F]-AV-1451 SUVR and thickness for each of the regions that composed the AD cortical signature. We observed that the effect of the [^{18}F]-AV-1451 SUVR on

cortical thickness was not only significant for each region but was present in a particular order. Specifically, the magnitude of observed correlation decreased in the following order: the medial temporal, inferior temporal, lateral temporal or inferior parietal lobule, posterior medial parietal, and superior parietal lobule (Figure 1).

We assessed the interactive effect of Aβ status and [F-18]-AV-1451 SUVR on volumetric measurements. An interaction between Aβ status and the hippocampal [^{18}F]-AV-1451 SUVR was observed for the hippocampal volume. Within Aβ+ participants, the hippocampal [^{18}F]-AV-1451 SUVR was negatively correlated with the hippocampal volume (R^2 = 0.55; P < .001). The hippocampal [^{18}F]-AV-1451 SUVR explained 31% of the variance in the hippocampal volume after accounting for age and CDR status (P = .02). Within Aβ− participants, no association was observed between hippocampal [^{18}F]-AV-1451 SUVR and volume (R^2 = 0; P = .97).

An interactive effect was not observed between Aβ status and AD cortical signature [^{18}F]-AV-1451 SUVR for AD signature cortical thickness. The [^{18}F]-AV-1451 SUVR in AD cortical signature regions explained 18% of the variance in AD cortical signature thickness after accounting for age and CDR status (P = .007). In addition, no interactive effects were seen between Aβ status and regional [^{18}F]-AV-1451 SUVR for each of the regions of interest that composed the AD cortical signature. Across the 6 AD cortical signature regions, [^{18}F]-AV-1451 SUVR explained different proportions of the variance in thickness after accounting for age and CDR status. In particular, across the 6 AD cortical signature regions of interest, the variance in thickness explained by [^{18}F]-AV-1451 SUVR exhibited a similar descending order as seen in Figure 1A.

In addition, to ensure that the topography of the AD cortical signature adequately represented the primary areas that demonstrate an association between [^{18}F]-AV-1451 SUVR and cortical thickness, we performed a vertex analysis for the entire cortical mantle. We found that an increase in the [^{18}F]-AV-1451 SUVR was associated with reduced cortical thickness in the medial temporal, inferior temporal, lateral temporal, and medial and lateral parietal areas (Figure 1B). Our vertexwise analysis suggested that [^{18}F]-AV-1451–related cortical thinning was topographically similar to AD cortical signature regions.

Discussion

Binding of [^{18}F]-AV-1451 in the hippocampus and AD cortical signature regions accurately distinguished AD from CN participants. This finding is consistent with other neuropathologic studies suggesting that tau burden is closely correlated with disease progression.[5] Moreover, the receiver operating characteristic–derived cutoff (ie, AD signature [^{18}F]-AV-1451 SUVR, 1.19) and the gaussian mixture model classified Aβ+ CN participants into low vs high tau groups. The classification using the [^{18}F]-AV-1451 SUVR is consistent with the neuropathologic description of preclinical AD, in which antemortem CN cases have been shown[4] to have neocortical accumulation of plaques and neurofibrillary tangles that is similar to very mild AD. Longitudinal studies are required for prognosis of this classification and comparison with stage 2 of preclinical AD defined by CSF tau, volumetric MRI, or fluorodeoxyglucose PET.

Sequential changes in neurodegenerative markers occur with AD progression.[24,37] Specifically, CSF tau (ptau as well) becomes abnormal before volumetric MRI in preclinical AD[37] (but see other reports[20,38]). Volumetric MRI has been shown[24,37] to be more dynamic than CSF tau/ptau across clinical AD. We assessed cross-sectional changes in CSF $ptau_{181}$, volumetrics, and [^{18}F]-AV-1451 with increasing stages of AD. Consistent with the reported sequence,[24,37] changes in CSF $ptau_{181}$ and volumetic MRI were primarily seen with the presence of preclinical and clinical AD, respectively. More important, [^{18}F]-AV-1451 binding from AD cortical signature regions was elevated in both the preclinical and clinical stages of AD. Therefore, [^{18}F]-AV-1451 may detect a wider range of AD neurodegeneration than CSF tau or volumetric MRI.

Neurofibrillary tangles are commonly detected in the hippocampus and adjacent medial temporal cortices at autopsy in elderly participants (>60 years).[4,39,40] Consistent with this observation,[4,39,40] we found that hippocampal [^{18}F]-AV-1451 levels were similar between Aβ+ and Aβ− participants. However, Aβ status had a dramatic effect on the association between hippocampal neurofibrillary tangles and volume. In the absence of Aβ, no association was seen between hippocampal [^{18}F]-AV-1451 binding and volume. Given that hippocampal volume is a well-validated measure for AD neurodegeneration,[41] this result supports a view[27] that, in the absence of Aβ, age-related hippocampal tauopathy may be insufficient for the neurodegenerative process that leads to AD. However, the presence of Aβ was associated with a strong inverse association between hippocampal tauopathy and volume. This result suggests an intriguing hypothesis in which Aβ transforms age-related hippocampal tau to a more toxic species that damages neurons and synapses. Further work exploring the molecular mechanisms underlying this result is needed.

Consistent with recent work,[17] we observed that cortical [^{18}F]-AV-1451 binding, measured from AD cortical signature regions, was elevated with the presence of Aβ. Furthermore, we found that elevated [^{18}F]-AV-1451 binding was associated with cortical thinning in AD cortical signature regions. However, Aβ+ status had no effect on AD signature cortical thickness or the association between AD signature cortical thickness and [^{18}F]-AV-1451 binding. These results collectively support the hypothesis that Aβ acts as an initiator in a pathogenic cascade that triggers the spread of tauopathy into the neocortex, which in turn leads to cortical neurodegeneration.[25] In addition, across AD cortical signature regions, the degree to which [^{18}F]-AV-1451 binding was related to cortical thinning that tracked the same topographic order of neurofibrillary tangle spread seen at autopsy.[1] This result may provide in vivo evidence that tau-related neurodegeneration evolves in a spatially ordered fashion. The biology underlying the spread of tauopathy remains unclear. Experimental evidence suggests that tau proteins transfer between neurons via synaptic connection.[42] Further studies are needed to understand where and how Aβ facilitates the transsynaptic transfer of misfolded tau proteins.

At present, tau imaging is in early developmental staging. Tau imaging work generally has limited sample size. In particular, we

classified the present cohort into disease stage–defined groups, which led to smaller samples of individual cohorts. In addition, the effects of off-target binding to choroid plexus might not be completely removed by partial volume correction or regression procedure. Although observed disease stage–related changes in [^{18}F]-AV-1451 binding were consistent with neuropathologic reports, these results need to be replicated in larger cohorts using tracers that are more specific to tauopathy.

Conclusions

Overall, our work suggests that [^{18}F]-AV-1451 is a valuable tool in tracking the continuum of the neurodegenerative process that ranges from the preclinical to clinical phase of AD. In particular, [^{18}F]-AV-1451 binding sampled from AD cortical signature regions may offer a pathologically plausible means to stage preclinical AD. Our work also suggests that interactions between Aβ and tau are the key for neurodegeneration due to AD. In the hippocampus, Aβ likely transforms preexisting tauopathy to a more toxic species that results in neuronal injury. In the cerebral cortex, Aβ may intensify the spread of tauopathy, which in turn leads to neuronal loss that follows a topography that is similar to the observed spread of neurofibrillary tangles at autopsy. In the absence of Aβ, tauopathy may be confined to the hippocampus and adjacent medial temporal cortices and is insufficient for hippocampal degeneration that leads to AD.

ARTICLE INFORMATION

Accepted for Publication: May 3, 2016.

Published Online: July 25, 2016. doi:10.1001/jamaneurol.2016.2078.

Author Contributions: Dr Ances had full access to all the data in the study and takes responsibility for the integrity of the data and the accuracy of the data analysis.
Study concept and design: Wang, Benzinger, Aldea, McConathy, Cairns, Ances.
Acquisition, analysis, or interpretation of data: Wang, Benzinger, Su, Christensen, Friedrichsen, Aldea, McConathy, Cairns, Fagan, Morris.
Drafting of the manuscript: Wang, Aldea.
Critical revision of the manuscript for important intellectual content: Wang, Benzinger, Su, Christensen, Friedrichsen, McConathy, Cairns, Fagan, Morris, Ances.
Statistical analysis: Wang, Friedrichsen.
Obtained funding: Benzinger, Morris, Ances.
Administrative, technical, or material support: Benzinger, Su, Christensen, Friedrichsen, Aldea, McConathy, Cairns, Fagan, Ances.
Study supervision: Benzinger, Morris, Ances.

Conflict of Interest Disclosures: Dr Fagan is a member of the scientific advisory boards of IBL International and Roche and is a consultant for AbbVie, Novartis, and DiamiR. Drs Benzinger and Morris and are currently participating in a clinical trial of antidementia drugs: A4 (The Anti-Amyloid Treatment in Asymptomatic Alzheimer's Disease) trial. Dr Benzinger also participates in the Dominantly Inherited Alzheimer Network Trials Unit and in clinical trials sponsored by Eli Lilly/Avid Radiopharmaceuticals. Dr Morris has served as a consultant for Lilly USA and Takeda Pharmaceuticals. Drs Benzinger and Morris receive research support from Eli Lilly/Avid Radiopharmaceuticals. Dr McConathy has served as a consultant for Eli Lilly/Avid Radiopharmaceuticals, GE Healthcare, and Siemens Healthcare. No other disclosures were reported.

Funding/Support: Funding for the study was received from Knight Alzheimer's Disease Research Center (ADRC) pilot grant 3255 ADRC 26 (Dr Ances); National Institute of Mental Health grant R21MH099979 (Dr Ances); National Institute of Nursing Research grants R01NR014449, R01NR012657, and R01NR012907) (Dr Ances); Alzheimer's Association (Dr Ances), National Institute on Aging grants P01AG026276, P01AG03991, and P50 AG05681 (Dr Morris); the generous support of Fred Simmons and Olga Mohan; the Barnes-Jewish Hospital Foundation; the Hope Center for Neurological Disorders; and the Paula and Rodger O. Riney Fund. Research reported in this article was also supported by the Washington University Institute of Clinical and Translational Sciences grant UL1 TR000448 from the National Center for Advancing Translational Sciences of the National Institutes of Health. Support from Avid Radiopharmaceuticals (a wholly owned subsidiary of Eli Lilly) included provision of the precursor to AV-1451, radiochemistry support, and cross-referencing of the investigational new drug application.

Role of the Funder/Sponsor: The funding organizations had no role in the design and conduct of the study; collection, management, analysis, and interpretation of the data; preparation, review, or approval of the manuscript; and decision to submit the manuscript for publication.

Disclaimer: The content is solely the responsibility of the authors and does not necessarily represent the official views of the National Institutes of Health.

Additional Contributions: The Knight ADRC Clinical Core for participant assessments and the Imaging Core provided magnetic resonance imaging and positron emission tomography data acquisition and preprocessing, and the Biomarker Core conducted cerebrospinal fluid analyses. We thank all of our research participants and their families. There was no additional financial compensation.

REFERENCES

1. Braak H, Braak E. Neuropathological stageing of Alzheimer-related changes. *Acta Neuropathol*. 1991;82(4):239-259.

2. Braak H, Alafuzoff I, Arzberger T, Kretzschmar H, Del Tredici K. Staging of Alzheimer disease-associated neurofibrillary pathology using paraffin sections and immunocytochemistry. *Acta Neuropathol*. 2006;112(4):389-404.

3. Thal DR, Rüb U, Orantes M, Braak H. Phases of Aβ-deposition in the human brain and its relevance for the development of AD. *Neurology*. 2002;58(12):1791-1800.

4. Price JL, Morris JC. Tangles and plaques in nondemented aging and "preclinical" Alzheimer's disease. *Ann Neurol*. 1999;45(3):358-368.

5. Delacourte A, David JP, Sergeant N, et al. The biochemical pathway of neurofibrillary degeneration in aging and Alzheimer's disease. *Neurology*. 1999;52(6):1158-1165.

6. Fagan AM, Mintun MA, Mach RH, et al. Inverse relation between in vivo amyloid imaging load and cerebrospinal fluid Aβ42 in humans. *Ann Neurol*. 2006;59(3):512-519.

7. Klunk WE, Engler H, Nordberg A, et al. Imaging brain amyloid in Alzheimer's disease with Pittsburgh Compound-B. *Ann Neurol*. 2004;55(3):306-319.

8. Buerger K, Ewers M, Pirttilä T, et al. CSF phosphorylated tau protein correlates with neocortical neurofibrillary pathology in Alzheimer's disease. *Brain*. 2006;129(pt 11):3035-3041.

9. Sperling RA, Aisen PS, Beckett LA, et al. Toward defining the preclinical stages of Alzheimer's disease: recommendations from the National Institute on Aging-Alzheimer's Association workgroups on diagnostic guidelines for Alzheimer's disease. *Alzheimers Dement*. 2011;7(3):280-292.

10. Chien DT, Bahri S, Szardenings AK, et al. Early clinical PET imaging results with the novel PHF-tau radioligand [F-18]-T807. *J Alzheimers Dis*. 2013;34(2):457-468.

11. Xia CF, Arteaga J, Chen G, et al. [^{18}F]T807, a novel tau positron emission tomography imaging agent for Alzheimer's disease. *Alzheimers Dement*. 2013;9(6):666-676.

12. Maruyama M, Shimada H, Suhara T, et al. Imaging of tau pathology in a tauopathy mouse model and in Alzheimer patients compared to normal controls. *Neuron*. 2013;79(6):1094-1108.

13. Okamura N, Furumoto S, Fodero-Tavoletti MT, et al. Non-invasive assessment of Alzheimer's disease neurofibrillary pathology using ^{18}F-THK5105 PET. *Brain*. 2014;137(pt 6):1762-1771.

14. Marquié M, Normandin MD, Vanderburg CR, et al. Validating novel tau positron emission tomography tracer [F-18]-AV-1451 (T807) on postmortem brain tissue. *Ann Neurol*. 2015;78(5):787-800.

15. Villemagne VL, Fodero-Tavoletti MT, Masters CL, Rowe CC. Tau imaging: early progress and future directions. *Lancet Neurol*. 2015;14(1):114-124.

16. Ossenkoppele R, Schonhaut DR, Baker SL, et al. Tau, amyloid, and hypometabolism in a patient with posterior cortical atrophy. *Ann Neurol*. 2015;77(2):338-342.

17. Johnson KA, Schultz A, Betensky RA, et al. Tau positron emission tomographic imaging in aging and early Alzheimer's disease. *Ann Neurol*. 2016;79(1):110-119.

18. Schöll M, Lockhart SN, Schonhaut DR, et al. PET imaging of tau deposition in the aging human brain. *Neuron*. 2016;89(5):971-982.

19. Schwarz AJ, Yu P, Miller BB, et al. Regional profiles of the candidate tau PET ligand ^{18}F-AV-1451 recapitulate key features of Braak histopathological stages. *Brain*. 2016;139(pt 5):1539-1550.

20. Dickerson BC, Bakkour A, Salat DH, et al. The cortical signature of Alzheimer's disease: regionally specific cortical thinning relates to symptom severity in very mild to mild AD dementia and is detectable in asymptomatic amyloid-positive individuals. *Cereb Cortex*. 2009;19(3):497-510.

21. Vemuri P, Whitwell JL, Kantarci K, et al. Antemortem MRI based STructural Abnormality iNDex (STAND)-scores correlate with postmortem Braak neurofibrillary tangle stage. *Neuroimage*. 2008;42(2):559-567.

22. Wang L, Benzinger TL, Hassenstab J, et al. Spatially distinct atrophy is linked to β-amyloid and tau in preclinical Alzheimer disease. *Neurology*. 2015;84(12):1254-1260.

23. Jagust W. Time for tau. *Brain*. 2014;137(pt 6):1570-1571.

24. Jack CR Jr, Knopman DS, Jagust WJ, et al. Tracking pathophysiological processes in Alzheimer's disease: an updated hypothetical model of dynamic biomarkers. *Lancet Neurol*. 2013;12(2):207-216.

25. Musiek ES, Holtzman DM. Three dimensions of the amyloid hypothesis: time, space and "wingmen." *Nat Neurosci*. 2015;18(6):800-806.

26. Sperling R, Mormino E, Johnson K. The evolution of preclinical Alzheimer's disease: implications for prevention trials. *Neuron*. 2014;84(3):608-622.

27. Delacourte A, Sergeant N, Wattez A, et al. Tau aggregation in the hippocampal formation: an ageing or a pathological process? *Exp Gerontol*. 2002;37(10-11):1291-1296.

28. Lace G, Savva GM, Forster G, et al; MRC-CFAS. Hippocampal tau pathology is related to neuroanatomical connections: an ageing population-based study. *Brain*. 2009;132(pt 5):1324-1334.

29. Jack CR Jr, Wiste HJ, Weigand SD, et al. Amyloid-first and neurodegeneration-first profiles characterize incident amyloid PET positivity. *Neurology*. 2013;81(20):1732-1740.

30. Crary JF, Trojanowski JQ, Schneider JA, et al. Primary age-related tauopathy (PART): a common pathology associated with human aging. *Acta Neuropathol*. 2014;128(6):755-766.

31. Berg L, McKeel DW Jr, Miller JP, et al. Clinicopathologic studies in cognitively healthy aging and Alzheimer's disease: relation of histologic markers to dementia severity, age, sex, and apolipoprotein E genotype. *Arch Neurol*. 1998;55(3):326-335.

32. Morris JC. The Clinical Dementia Rating (CDR): current version and scoring rules. *Neurology*. 1993;43(11):2412-2414.

33. Morris JC, Weintraub S, Chui HC, et al. The Uniform Data Set (UDS): clinical and cognitive variables and descriptive data from Alzheimer Disease Centers. *Alzheimer Dis Assoc Disord*. 2006;20(4):210-216.

34. Su Y, Blazey TM, Snyder AZ, et al. Quantitative amyloid imaging using image-derived arterial input function. *PLoS One*. 2015;10(4):e0122920.

35. Su Y, Blazey TM, Snyder AZ, et al; Dominantly Inherited Alzheimer Network. Partial volume correction in quantitative amyloid imaging. *Neuroimage*. 2015;107:55-64.

36. Team RDC. *R: A Language and Environment for Statistical Computing*. Vienna, Austria: R Foundation for Statistical Computing; 2008.

37. Jack CR Jr, Vemuri P, Wiste HJ, et al; Alzheimer's Disease Neuroimaging Initiative. Evidence for ordering of Alzheimer disease biomarkers. *Arch Neurol*. 2011;68(12):1526-1535.

38. Chételat G, Villemagne VL, Villain N, et al; AIBL Research Group. Accelerated cortical atrophy in cognitively normal elderly with high β-amyloid deposition. *Neurology*. 2012;78(7):477-484.

39. Braak H, Braak E. Frequency of stages of Alzheimer-related lesions in different age categories. *Neurobiol Aging*. 1997;18(4):351-357.

40. Nelson PT, Alafuzoff I, Bigio EH, et al. Correlation of Alzheimer disease neuropathologic changes with cognitive status: a review of the literature. *J Neuropathol Exp Neurol*. 2012;71(5):362-381.

41. Jack CR Jr, Barkhof F, Bernstein MA, et al. Steps to standardization and validation of hippocampal volumetry as a biomarker in clinical trials and diagnostic criterion for Alzheimer's disease. *Alzheimers Dement*. 2011;7(4):474-485.

42. de Calignon A, Polydoro M, Suárez-Calvet M, et al. Propagation of tau pathology in a model of early Alzheimer's disease. *Neuron*. 2012;73(4):685-697.